HHS Public Access

Author manuscript

Structure. Author manuscript; available in PMC 2015 December 02.

Published in final edited form as:

Structure. 2014 December 2; 22(12): 1744–1753. doi:10.1016/j.str.2014.10.001.

The TLQP-21 Peptide Activates the G-protein-coupled receptor C3aR1 via a *Folding-upon-Binding* Mechanism

Cheryl Cero[#1], **Vitaly V. Vostrikov**[#2], **Raffaello Verardi**[#2], **Cinzia Severini**[3], **Tata Gopinath**[2], **Patrick D. Braun**[4], **Maria F. Sassano**[5], **Allison Gurney**[1], **Bryan L. Roth**[5], **Lucy Vulchanova**[7], **Roberta Possenti**[3,6], **Gianluigi Veglia**[2,*], and **Alessandro Bartolomucci**[1,*]

[1] Department of Integrative Biology and Physiology, University of Minnesota, Minneapolis, MN 55455

[2] Department of Biochemistry, Molecular Biology and Biophysics, University of Minnesota, Minneapolis, MN 55455

[3] Institute of Cell Biology and Neurobiology, National Research Council, Rome, Italy 00143

[4] Department of Pharmaceutics, University of Minnesota, Minneapolis, MN 55455

[5] Department of Pharmacology and National Institute of Mental Health Psychoactive Drug Screening Program School of Medicine, University of North Carolina, Chapel Hill, NC 27599.

[6] Department of Medicine of System, University of Rome 'Tor Vergata', Rome, Italy 00133.

[7] Department of Veterinary and Biomedical Sciences, University of Minnesota, Saint Paul, MN 55108.

[#] These authors contributed equally to this work.

SUMMARY

TLQP-21, a VGF-encoded peptide is emerging as a novel target for obesity-associated disorders. TLQP-21 is found in the sympathetic nerve terminals in the adipose tissue and targets the G-protein-coupled-receptor (GPCR) Complement-3a-Receptor1 (C3aR1). So far, the mechanisms of TLQP-21-induced receptor activation remained unexplored. Here, we report that TLQP-21 is intrinsically disordered and undergoes a *disorder-to-order* transition, adopting an α-helical conformation, upon targeting cells expressing the C3aR1. We determined that the hot spots for TLQP-21 are located at the C-terminus, with mutations in the last four amino acids progressively reducing the bioactivity and, a single site mutation (R21A) or C-terminal amidation abolishing its

[*] Correspondence should be addressed to: Alessandro Bartolomucci, Ph.D., Department of Integrative Biology and Physiology University of Minnesota, 2231 6th St. SE, Minneapolis, MN 55455. Phone:+1- 612-626-7006; FAX: +1612-625-5149; abartolo@umn.edu; or Gianluigi Veglia, PhD. Department of Biochemistry, Molecular Biology & Biophysics University of Minnesota, 321 Church Street SE, Minneapolis, MN 55455. Phone: (612) 625 0758, vegli001@umn.edu..

AUTHOR CONTRIBUTIONS

CC,VV,RV,CS,TG,PDB, MFS,BLR,AG,LV,PR,GV,AB, performed experiments and analyzed data; LV,RP,GV,AB, conceptualized the experiments; GV, AB wrote the manuscript with input from all coauthors.

function completely. Interestingly, the human TLQP-21 sequence carrying a S20A substitution activates the human C3aR1 receptor with lower potency compared to the rodent sequence. These studies reveal the mechanism of action of TLQP-21 and provide molecular templates for designing agonists and antagonists to modulate C3aR1 functions.

Keywords

Adipocyte; Alanine scanning; Lipolysis; Solid-state NMR; VGF

INTRODUCTION

The *Vgf* gene is a member of the extended granin family of peptide-precursor proteins that encodes a 615 amino acid pro-peptide (617 in rodents) (Bartolomucci et al., 2001). This pro-peptide is processed to yield several bioactive fragments, with at least eight possessing non-redundant biological functions (Bartolomucci et al., 2011; Hahm et al., 1999). Due to their involvement in the pathophysiology of human diseases such as psychiatric, neurological and metabolic disorders as well as several tumors, VGF peptide fragments are also being investigated as possible disease biomarkers (Bartolomucci et al., 2011). The best studied fragment is the C-terminal internal peptide designated TLQP-21, whose sequence and function we have identified and extensively characterized (Bartolomucci et al., 2006). TLQP-21 is a multifunctional peptide that regulates energy balance (Bartolomucci et al., 2006, Jethwa et al., 2007, Possenti et al., 2012), glucose metabolism (Stephens et al., 2012), gastric function (Severini et al., 2009), nociception (Rizzi et al., 2007, Chen et al., 2013, Fairbanks et al., 2014), blood pressure regulation (Fargali et al., 2014), reproduction (Aguilar et al., 2013) and stress (Razzoli et al., 2012). Importantly, it was found that a central infusion of TLQP-21 increases energy expenditure and prevents obesity in rodents (Bartolomucci et al., 2006, Jethwa et al., 2007). Additionally, chronic peripheral infusions of TLQP-21 in obese rodents led to decreased adipocyte diameter (Possenti et al., 2012) improved hypertension (Fargali et al., 2014) and diabetes (Stephens et al., 2012), making it an important target to counteract obesity-associated disorders. However, the molecular mechanisms of TLQP-21 function are still largely unknown. The recent discovery that TLQP-21 directly targets the Complement 3a receptor 1 (C3aR1) has reinvigorated both physiological and pharmacological interest for this peptide as a potential drug target (Hannedouche et al., 2013). C3aR1 is a member of the GPCR superfamily, characterized by seven transmembrane domains and a large second extracellular loop (Klos et al., 2013, Roglic et al., 1996). While its role in the innate immune response is well established, C3aR1 is now emerging with a much broader pattern of expressions in different tissues and functions involving cell metabolism (e.g. Mamane et al., 2009; Lo et al., 2014). In obesity, a significant increase of adipose-tissue specific C3aR1 expression has been found (Mamane et al., 2009), with concomitant increase of TLQP-21 binding affinity (Possenti et al., 2012). Additionally, knockout studies targeting C3, C3aR1 and VGF suggest direct involvement of the C3aR1 receptor in both adiposity and energy balance (Mamane et al., 2009, Hahm et al., 1999, 2001, Roy et al., 2008, Fargali et al., 2012, Watson et al., 2005). Here, we used solid-state NMR spectroscopy in combination with photoaffinity labeling, biological assays as well as alanine-scanning mutagenesis to elucidate the structural determinants of TLQP-21

binding to C3aR1. We studied the binding of TLQP-21 to cells expressing the receptor as well as receptor knockout cells. We found that the TLQP-21 peptide is intrinsically disordered but adopts an ordered helical conformation upon interacting with cells expressing the C3aR1 receptor. Furthermore, we determined that the C-terminal domain of the peptide comprises the hot-spots for its biological function, with the R21A mutation able to abrogate TLQP-21 activity completely. Finally, we found that the human sequence of TLQP-21 carrying a S20A substitution activates human C3aR1 receptor with lower potency than the rodent sequence. Overall, these studies reveal a folding-upon-binding mechanism for the activation of the C3aR1 receptor by the TLQP-21 peptide, and identify the hot-spots to tune its biological function.

RESULTS

TLQP-21 targets the C3aR1 receptor

To establish the selective binding of the TLQP-21 to the C3aR1 receptor, we carried out photoaffinity labeling experiments. First, we synthesized a biotin-conjugated TLQP-21 peptide, substituting F13 with a benzophenone derivative; we then incubated the peptide with both 3T3L1 and CHO cells which express the C3aR1 (**Figure S1** and (Possenti et al., 2012, Choy et al., 1995, Cassina et al., 2013)). Upon UV irradiation of the reaction mixture, the modified peptide consistently cross-linked with a protein running at approximately 55 kDa on the SDS-PAGE, corresponding to the nominal molecular weight of the C3aR1 receptor (Klos et al., 2013, Roglic et al., 1996) (**Figure 1A**). To test the binding specificity of the TLQP-21 for the C3aR1 receptor, we carried out the same reaction in the presence of SB290157, a well-documented C3aR1antagonist (Ames et al., 2001). In the presence of the antagonist, we observed a substantial reduction in cross-linking efficiency (**Figure 1B**), indicating that SB290157 competes with TLQP-21 binding to the C3aR1 receptor.

To provide additional evidence that TLQP-21 targets the C3aR1, we used a β-arrestin recruitment assay in HTLA cells transfected with the C3aR1 receptor (Lin et al., 2013). We found that the EC_{50} for mouse TLQP-21 is approximately 3 times lower than that of C3a and the EC_{50} for the human TLQP-21 is approximately 22 times lower than C3a (**Figure 1C**; EC_{50}, C3a=3.0μM; mouse TLQP-21=10.3μM; human TLQP-21=68.8μM), indicating that both human and mouse TLQP-21 species are active toward human C3aR1, although with different potency.

TLQP-21 undergoes a *disorder-to-order* transition upon binding C3aR1

Secondary structure predictions showed that the TLQP-21 sequence has a low propensity to form a well-order α-helix (Garcia et al., 2005) (**Figure S2**). Accordingly, solution NMR experiments in aqueous solutions showed that the peptide is essentially unstructured, with a chemical shift index typical of random coil conformations (**Figure S2**). Addition of the helical-promoting solvent trifluoroethanol or dodecyl phosphocholine micelles left the resonances of the peptide essentially unperturbed, excluding its propensity to adopt an ordered conformation in membrane mimicking environments (**Figure S2**). We then tested the peptide's interactions with lipid membranes using magic angle spinning (MAS) solid-state NMR spectroscopy. To visualize the peptide, we synthesized three different TLQP-21

analogs with ^{15}N, ^{13}C labels interspersed throughout its primary sequence: TLQP-21-*ALP*, labeled at A_{16}, L_{17}, P_{18}; TLQP-21-*PAR*, labeled at P_4, A_6, R_9; and TLQP-21-*PARRPA*, labeled P_4, A_6, R_9, R_{11}, P_{19}, A_{20}. (**Figure S3**). We performed two different experiments: the refocused INEPT (rINEPT) experiment, which is sensitive to more dynamic regions of proteins (Fyfe et al., 1995), and cross-polarization (CP) experiments (Engelke and Steuernagel 2007), which detects more rigid domains (**Figure S3**). The peptide was reconstituted with large unilamellar vesicles of DOPC:DOPE. Under these conditions, we did not observe any peptide resonances in the CP spectra, excluding a strong binding of the peptide to the membrane vesicles, and at the same time supporting the dynamic nature of the peptide. In contrast, the rINEPT experiment detected essentially all of the labeled sites, displaying a well-resolved spectrum of TLQP-21 with chemical shift values corresponding to the tabulated random coil values (http://www.bmrb.wisc.edu) (**Figure 2A,C,E** and **Figure S2D**). Taken with the solution NMR experiments, the solid-state NMR spectra showed that the peptide is intrinsically disordered in solution and does not have a strong tendency to associate with lipid bilayers. To test TLQP-21 binding under the native conditions rather than in a reconstituted system, we probed the peptide-receptor interactions by incubating the peptide with 3T3L1 cells that express C3aR1 (**Figure S1**). Under these conditions, TLQP-21 underwent a *disorder-to-order* transition (**Figure 2B,F,D**). Specifically, the chemical shifts of the Cα-Hα resonances changed significantly (**Figure 2G,H**), consistent with a structural transition from random coil to α-helical conformation (**Figure 3**). The experiment was repeated for three labeled TLQP-21 analogs spanning the core sequence, and in all cases we observed the same chemical shift transitions from random coil to helix (**Figure 2**).

To confirm the specificity of the binding under NMR conditions, we analyzed TLQP-21 binding in the presence of N^2-[(2,2-Diphenylethoxy)acetyl-L-Arginine (or SB290157), a potent inhibitor of C3aR1 that does not antagonize either C5aR or other GPCRs (Ames et al., 2001). Since the concentration of the receptor is unknown, we used 5 μM of the inhibitor. In the spectrum of *TLQP-PAR* (**Figure 4C**) we detected two conformations of the peptide: one with chemical shifts corresponding to the unfolded peptide, and a weaker set matching the helical structure. These data indicate that there is only a partial saturation of the receptor on the adipocytes with the SB290157 inhibitor. To circumvent this issue, we used splenocytes derived from either wild type mouse expressing C3aR1 receptor (Kwan et al., 2013), or from a C3aR1 knockout mouse. Again, for the wild type cells we observe the backbone chemical shifts matching those of the folded helical conformation (Figure 4E). Conversely, TLQP-21 incubated with the C3aR1 knockout splenocytes exhibits chemical shifts those of the unfolded structure (Figure 4F). Finally, although the N38 cell line has been proposed as a negative control for TLQP-21 activity (Cassina et al., 2013), we detected significant expression of the C3aR1 receptor using QPCR (**Figure S1**). As a result, we have observed binding of the TLQP-21 peptide to the receptor with concomitant transitions from disordered to helical conformation (**Figure S4**).

Determination of the hot spots for TLQP-21 biological function

After establishing the structural determinant of TLQP-21 binding to C3aR1, we sought to identify the hot spots for the peptide activity. The primary amino acid sequence of murine TLQP-21 (TLQPPASSRRRHFHHALPPAR) corresponds to amino acids 556–576 of the

VGF pro-peptide (Bartolomucci et al., 2006, 2011). One of the best characterized bioassays for TLQP-21 activity is the contraction of stomach fundus strips (Severini et al., 2009). At a dose of 3μM TLQP-21 induces up to ~69% of the corresponding contraction promoted by acetylcholine. To elucidate the hot spots responsible for optimal biological activity, we synthesized and tested the biological response of two truncated analogs of the TLQP-21 peptide: one without the C-terminal sequence (TLQP-11), and the second without the N-terminus (HFHH-10). We found that TLQP-11 is essentially inactive, with zero response at concentrations up to 10μM (**Table 1**), while HFHH-10 induced a modest biological activity, with ~3% response at a concentration of 3μM, 62% at 6μM, and 75% at 10μM. These experiments suggest that the hot spots for biological activity are situated at the C-terminus, and demonstrate that the entire peptide sequence is required for its optimal activity. We next performed Ala-scanning mutagenesis (Morrison and Weiss 2001) on the C-terminal portion of TLQP-21. We found that mutations of endogenous amino acids with Ala had no significant effects, with the exception of the four C-terminal amino acids. Specifically, the P18A mutant showed partial biological function with ~65% activity at 3μM. The P19A mutant showed only residual activity with 19% at 3μM (and 35% at 6μM) (**Table 1; Figure S5**). Interestingly, the human TLQP-21, in which Ser is in position 20 (Ala for the rodent sequence), showed limited biological activity toward the rodent receptor with ~20% at 3μM compared to the mouse sequence (**Table 1**), a finding which is in line with the β-arrestin activity assays reported in **Figure 1c**. Importantly, the R21A mutant resulted in a complete loss of activity (**Table 1; Figure S5**), even after increasing the dose up to 10μM. The inactive R21A mutant does not block the activity of a subsequent infusion of TLQP-21, suggesting that it does not behave as a C3aR1 antagonist (**Table 1; Figure S5**). Note that under our conditions the biological activity elicited by TLQP-21 is similar to that of the C3aR1 agonist $C3a_{70\text{-}77}$ (Hugli and Erickson 1977), with 3μM TLQP-21 and $C3a_{70\text{-}77}$ causing approximately 69% and 55% contraction of fundus strips, respectively, relative to acetylcholine (**Figure S5**). Finally, we investigated the effects of capping the TLQP-21 C-terminus via amidation. Although this post-translational modification is not observed for the TLQP-21 peptide *in vivo* (Bartolomucci et al., 2006), it represents a pre-requisite for the activity of several other hormonal peptides such as CRH (Vale et al., 1981), and it increases the stability of several synthetic peptides (Adessi and Soto 2002). Upon C-terminal amidation, the TLQP-21 peptide is completely inactivated (**Table 1**), suggesting that the free carboxylic group is necessary for activity.

Arginine 21 is essential for TLQP-21 lipolysis in 3T3L1 adipocytes

The above results support a central role of the C-terminal Arg for TLQP-21 activity. To further understand the function of TLQP-21, we assessed the pro-lipolytic effect of TLQP-21 in 3T3L1 adipocytes and compared it to the R21A mutant. We found that TLQP-21 does not increase lipolysis *per se* (**Figure 5A; Figure S6**), but enhances isoproterenol-induced lipolysis in a dose-dependent manner (**Figure 5A**). These results are in agreement with our previous results obtained with mouse adipocytes (Possenti et al., 2012). In contrast, we found that the R21A mutant does not potentiate isoproterenol-induced lipolysis (**Figure 5B**) or AMPK phosphorylation (Possenti et al., 2012) **(Figure S6**). These results underscore the role of TLQP-21 as an enhancer of βARs-induced lipolysis and highlight the critical role of Arg-21 for activating C3aR1. Importantly, NMR spectra of the

R21A mutant (labeled with ^{13}C and ^{15}N at A_{16}, L_{17} and P_{18}) in the presence of 3T3L1 cells show a conformational transition similar to that of the wild-type peptide (**Figure 5C**). Therefore, the loss-of-function character of the inactive mutant is probably due to changes in the electrostatic interactions at the C-terminal portion of the peptide. The latter is supported by the chemical structure of C3a (Hugli and Erickson 1977), by the analogous mutations at R77 of C3a (Nattesheim et al., 1988), as well as the chemical structure of the C3aR1 antagonist SB290157, which includes a hydrophobic N-terminal diphenylethoxy group linked to the acetyl-L-Arg moiety (Ames et al., 2001) that closely mimics the C-terminal residues of the TLQP-21 peptide.

DISCUSSION

The role of the TLQP-21 neuropeptide in the pathophysiology of gastrointestinal and metabolic functions has been recognized by several independent studies (Bartolomucci et al., 2011). Despite this, the molecular mechanisms for eliciting TLQP-21 function have remained elusive until a recent study identified the C3aR1 receptor as the target for TLQP-21 (Hannedouche et al., 2013). Indeed, our photoaffinity labeling and β-arrestin assays (**Figure 1**) data support these previous studies, showing that TLQP-21 cross-links with the C3aR1 receptor selectively. A second putative receptor for TLQP-21, the globular head of C1q has been recently described (Chen et al., 2013). Published (Possenti et al., 2012, Hannedouche et al., 2013, Passina et al., 2013) and current data do not support a second binding site in either CHO or 3T3L1 cells (**Figure 1**) and there is no apparent structural/functional similarity between TLQP-21 and the predicted C1q ligands (Gaboriaud et al., 2003).

Importantly, the NMR measurements demonstrated that the peptide is intrinsically disordered in solution and does not assume an ordered conformation upon addition of helical-inducing environments. However, when incubated with cells expressing C3aR1, the TLQP-21 peptide undergoes a folding-upon-binding transition, adopting a well-defined α-helical conformation (**Figure 3**). This structural transition does not occur in the presence of C3aR1-knockout cells and can be inhibited upon treatment of 3T3L1 cells with a selective and competitive antagonist of the C3aR1 receptor (Ames et al., 2001). Transition from a random coil to helix is a common mechanism for activating GPCRs of the secretin family (Shoichet and Kobilka 2012; Hollenstein et al., 2014; Parthier et al., 2009; Kamik et al., 2003). For these receptors, the ligand peptides have been found to be disordered in aqueous solutions, but adopted a structured helical conformation upon binding the extracellular domains of the receptors. The driving force for their binding and folding is the formation of amphipathic helices in which the hydrophobic residues embed into the binding site. At least six different examples have been reported in the literature, e.g. CRH, PACAP, Glucagon, GLP-1 etc, where the high-resolution structures have been solved by either NMR or X-ray crystallography (Pal et al., 2012). While the apparent mechanism of TLQP-21 helix folding is reminiscent of these peptide hormones, the chemical nature of this VGF-derived peptide is rather different, as TLQP-21 sequence is flanked by two pairs of proline residues at both termini. In the structural model derived from our chemical shift measurements, hydrophobic and hydrophilic residues are not segregated into two distinct faces of the helix; rather, the charges are interspersed throughout the peptide sequence (**Figure 3**). This suggests a

mechanism of recognition by the cognate receptor that is different from that of other peptide hormones for which a structural analysis has been conducted (Parthier et al., 2009). Furthermore, the C-terminus of peptides active at class B GPCR act as a docking site to initiate the helix formation, and the N-terminal residues are responsible for the activation of the receptors (Parthier et al., 2009; Karnik et al., 2003). Conversely peptides active at class A GPCR (including the C3aR1) (Beck-Sickinger et al., 1994; Neelamkavil, et al., 2005) as well as other peptides of the granin family (Bartolomucci et al., 2011), do not show a common binding mechanism. The hot spots for TLQP-21 activity reside at the C-terminus. In fact, alanine-scanning mutagenesis and two bioassays including fundus strip contraction and lipolysis in 3T3L1 cells showed that the C-terminal sequence (-$PPAR_{21}$) is central to TLQP-21 biological activity (**Table 1**). A similar situation is found for the C3a peptide, the first ligand ever identified for the C3aR1 (Nettesheim et al., 1988). In the absence of the receptor, the C3a peptide is organized in helical segments interrupted by short flexible loops that become less defined at residue 66 (Klos et al., 2013), while they adopt a significantly more ordered helical conformation in the crystal lattice (Nettesheim et al., 1988). As with TLQP-21, the C3a peptide's hot spots are located at the C-terminus, with R77 playing a critical function (Ames et al., 2001; Hugli and Erickson 1977; Nettesheim et al., 1988). By deleting the C-terminal R_{77} of C3a it is possible to ablate the peptide's function at C3aR1 completely, although the deletion mutant is still able to form an ordered helix (Nettesheim et al., 1988). A very similar result was obtained with TLQP-21. The R21A mutant of TLQP-21 is inactive while still undergoing an α-helix conformational change. A full understanding of the similarities in the mechanism of action of TLQP-21 and C3a is currently lacking. In CHO and HeK239 cells transfected with C3aR1, TLQP-21 binds the receptor with 100 fold lower affinity than C3a (Hannedouche et al., 2013), while both these ligands induce a similar contraction of gastric fundus strips (present data) and insulin release (Stephens et al., 2012; Lo et al., 2014). Conversely, mouse TLQP-21 enhances isoproterenol induced lipolysis in mouse adipocytes (Possenti et al., 2012) and murine 3T3L1 (present study), while in an heterologous system Lim et al (2013) showed that human serum C3a exerts the opposite effect in murine 3T3L1 cells. Finally, using mouse genetic it has been demonstrated that C3aR1 knockout mice are transiently resistant to diet-induced obesity and are protected from insulin resistance and liver steatosis (Mamane et al., 2009), similar to VGF knockout mice (Hahm et al., 1999, 2002). In conclusion, although the mechanism of binding to the C3aR1 receptor may appear similar for both TLQP-21 and C3a, differences in their primary sequences might account for the non-fully overlapping biological actions.

Another important finding of our investigation relates to the different function between human and rodent TLQP-21 sequences. A recent study reported that the human TLQP-21 sequence is 5-fold less potent toward the rodent C3aR1 than the corresponding rodent sequence (Hannedouche et al., 2013). Here, we tested the potency of these two peptides toward the human C3aR1 receptor and found that both human and mouse TLQP-21 sequences target the human receptor with different potency. Specifically, we found an EC_{50} for the mouse TLQP-21 approximately 3 times lower than the C3a peptide, while the corresponding EC_{50} for the human TLQP-21 is approximately 22 times lower (**Figure 1C**). The rodent (rat and mouse) and primate (human, chimpanzee, and macaque) TLQP-21 sequences differ by four amino acids (Bartolomucci et al 2011). However, Ala20 at the C-

terminus of the rodent peptide is substituted by Ser20 in the human sequence (**Table 1**), resulting in a mutation leading to a peptide with lower potency toward the primate and the rodent C3aR1. In support, mutations at the C-terminus of C3a reduce the affinity toward the human receptor (Klos et al., 2013). Interestingly, casoxin C (Tyr-Ile-Pro-Ile-Gln-Tyr-Val-Leu-Ser-Arg) and Oryzatensin (Gly-Tyr-Pro-Met-Tyr-Pro-Leu-Pro-Arg) are short bioactive peptides with sequence analogy with the human complement C3a(70-77) and substitution of Ala76 in C3a with either Ser or Pro respectively (Takahashi et al., 1996,1997). The biological activity of casoxin C and oryzatensin in the ileum-contraction assay is similar to $C3a_{70\text{-}77}$ but with lower potency (Takahashi et al., 1996, 1997). Overall these data suggests that, unlike the mutation of the Arg77/Arg21 which abrogate activity at the C3aR1 (see above), mutating the Ala76 in C3a and Ala20 in TLQP-21 could reduce their biological activity.

Based on our finding that TLQP-21 enhances lipolysis in adipocytes (**Figure 5** and (Possenti et al, 2012), the lower potency of the human TLQP-21 peptide might reduce the lipolytic potential of humans and may constitute one of the factors explaining human vulnerability to obesity. Conversely, the rodent peptide could represent a gain of function mutation with respect to the basal TLQP-21 activity toward the C3aR1 receptor and suggests possible point mutations for augmenting or reducing TLQP-21 potency in humans. The latter will have implications in the design of synthetic ligands that mimic α-helical conformations to target C3aR1 and activate lipolysis to treat obesity and obesity-related disorders. Synthetic molecules designed to target GPCRs have already been developed into potent agonists and antagonists by engineering lactam-bridges promoting α-helical structures (Neelamkavil et al., 2005; Ammoun et al., 2003; Grace et al. 2007; Murage et al., 2008; Pellecchia et al., 2008). The mouse TLQP-21 sequence represents a molecular template for designing new analogues of this peptide that can serve as agonists or antagonists for C3aR1 having important implication for obesity (Possenti et al., 2012) diabetes (Stephens et al., 2012), hypertension (Fargali et al., 2014), pain (Fairbanks et al., 2014) and potentially immune functions.

In summary, our results show a folding-upon-binding mechanism for TLQP-21 that activates the cognate C3aR1 receptor leading to enhanced lipolysis in adipocytes. Using a combination of spectroscopic and biological assays, we identified the hot spots for TLQP-21 function as residing at the C-terminal sequence of the peptide. C-terminal amidation or mutation of the basic arginine 21 residue obliterates peptide function, suggesting that both positive and negative electrostatic interactions at the C-terminus are necessary for biological activity.

This study represents a major step toward understanding the molecular mechanism for activation of TLQP-21 and paves the way for designing new agonists/antagonists to modulate the function of the C3aR1 receptor (Reid et al., 2013).

EXPERIMENTAL PROCEDURES

Peptide Synthesis and NMR spectroscopy.

General—All solvents used were HPLC grade. DIEA and TFA (peptide synthesis grade) were purchased from Fisher. Fmoc-protected amino acids, HBTU and HOBt, were purchased from AnaSpec. Preloaded Fmoc-AA-PEG-PS resins were purchased from Applied Biosystems. N-Fmoc isotopically labeled amino acids were purchased from Cambridge Isotope Laboratory. All other reagents were obtained from Sigma-Aldrich.

Synthesis of TLQP21—Starting with Fmoc-ARG−PEG-PS resin (initial loading 0.18 mmol/g), the 21 residue peptide TLQP21 was synthesized using Fmoc solid-phase synthesis on a CEM microwave peptide synthesizer. Side-chain protecting groups were 2,2,4,6,7-pentamethyldihydrobenzofuran-5-sulfonyl (Pbf) for Arg, triphenylmethyl (Trt) for Gln and His; and tert-butyl ethers (tBu) for Ser and Thr. Fmoc removal was achieved using a solution of 20% piperidine in DMF for 5 min. HBTU/HOBt/DIEA couplings required 7 min preactivation time following reaction times of 60 min. Upon reaction completion, the peptide-resin was deprotected and cleaved from the resin in batches of 200 mg with 2 mL of reagent B: 85% TFA, 5% phenol, 5% water, 5% TIPS for 4 h at 25 °C under mechanical stirring. The cleavage mixture was then filtered and the resin was washed with 2 mL reagent B. The cleaved peptide fractions were pooled together and precipitated by addition of 200 mL of cold diethyl ether and incubated for 24 h at 4 °C. The precipitated peptide was collected by centrifugation and washed three times with 200 mL of cold diethyl ether. The crude peptide pellet was dried under N_2 gas flow and dissolved in 50 mL of HPLC grade water. The crude peptide was filtered using a 0.2 μm polycarbonate filter and purified by reversed-phase HPLC on a C18 preparative column (Vydac, 218TP15 C18; 15 μm particles, 22 × 250 mm). The crude peptide solution was pre-equilibrated with 90% HPLC buffer A (99.9% water, 0.1% trifluoroacetic acid) with a flow rate of 10 mL/min. Peptide purification protocol consisted of: 1) linear gradient from 10% to 20% of buffer B (acetonitrile and 0.1% TFA) in 30 min and 2) subsequent isocratic elution. Fractions containing peptides were determined by analytical HPLC and pooled together before lyophilization. The molecular weight of the purified peptide was determined using ESI-MS (Agilent MSD SL Ion Trap). To remove TFA ions from the peptide, a simple exchange method was followed. Briefly, ion exchange resin (AG1-X8, Biorad) was prepared by washing with 10 vol of acetic acid (1.6M), followed by 10 vol of acetic acid (0.16M) and finally 5 vol of water. Purified peptide was dissolved in water at a concentration of approximately 4mg/mL and loaded onto the equilibrated resin. After one hour of incubation with shaking, the peptide was eluted from the resin by gravity and the resin was washed with water. Pooled peptide was aliquoted and the volume accurately measured. Samples from several aliquots were taken and submitted for amino acid analysis. Amino acid analysis was performed by the Protein Chemistry Laboratory (Texas A&M University). Ion-exchanged peptides were lyophilized and stored at −20 °C until use.

***NMR spectroscopy* (Veglia et al., 2012)—**For solution NMR experiments, the TLQP-21 peptide powder was dissolved in 120mM NaCl, 20mM NaHPO4, pH 7.0, 5% D_2O and transferred into a Shigemi tube. Heteronuclear single quantum (HSQC) and multiple

quantum (HMQC) correlation experiments were run to verify the labeling pattern in the isotopically labeled peptides. Magic angle spinning (MAS) samples were prepared by dissolving 0.5 to 1 mg of TLQP21 in 20 μL of 20 mM phosphate buffer, 120mM NaCl at pH 7.0. The suspension was vortexed and briefly sonicated. The mixture was transferred to a 3.2 mm thin wall rotor MAS rotor. 3T3L1, N38 or splenocytes were centrifuged in 1.5 mL microfuge tubes for 2 min at 13300 rpm. Twenty microliters of wet cell pellet were pipetted into a clean 0.5 mL microfuge tube and (where applicable) incubated with the selective C3aR1 antagonist SB 290157 for 3 hr at 4 °C. The cell pellet was added to 1.0 mg of lyophilized TLQP-21 powder, briefly vortexed and incubated at 37 °C overnight. The mixture was transferred to a 3.2 mm thin wall rotor MAS rotor. All of the NMR experiments were performed on a VNMRS spectrometer operating at a proton frequency of 600 MHz. One-dimensional ^{13}C spectra were acquired using a cross-polarization (CP) sequence with 1 ms contact time and spectral width of 100 kHz. The sample was spun at 8 kHz and the temperature was kept at 37 °C. Chemical shifts were assigned using refocused Insensitive Nuclei Enhanced by Polarization Transfer (rINEPT) and Total Through Bond Correlation Spectroscopy (TOBSY) experiments acquired using a BioMAS probe. Pulse widths were 5.5 μs (^{13}C, ^{15}N), 2.5 μs (^{1}H) with 100 kHz (direct ^{13}C dimension) and 3.33 kHz (indirect ^{1}H dimension) spectral widths. Typically, a total of 128 scans with 30 increments in the indirect dimension were acquired. The data were processed using NMRPipe and analyzed with Sparky software.

Secondary Structure Prediction—To analyze the secondary structure propensity of TLQP21 two programs were used: PredictProtein and JUFO. PredictProtein (www.predictprotein.org) is an automatic Internet service that includes software for the prediction of protein structure and function. The JUFO (http://www.meilerlab.org/index.php/servers/show?s_id=5) server provides a simultaneous prediction of secondary structure and trans-membrane spans from the protein sequence. It uses an Artificial Neural Network trained on databases of membrane proteins and soluble proteins.

Splenocyte isolation

BALB/cJ and C3aR1 knockout mice were euthanized with CO_2 and spleens were harvested. Spleens were placed in complete media and filtered to yield a single-cell suspension. Splenocytes were seeded at 1×10^6 cells/ml and stored in an incubator (37°C, 5% CO_2) for 4 hours until NMR sample preparation. Full details appear in the Supplementary Methods.

Gastric contraction assay

Wistar female rats (250-350 g; Charles River) were euthanized by inhalation of 75% CO_2 in air. The stomach was removed and washed in fresh Tyrode's solution as previously described (Severini et al., 2009) and the assay performed as previously described and detailed in the Supplementary Methods. Data were analyzed with unpaired t-tests. All animal experiments were approved by the Ethics Committee of the Italian Ministry of Health.

Receptor cross-linking experiment

Crosslink peptide with N-terminal biotin and benzoylphenylalanine (Bpa) substitution of H12 was purchased from AAPPTec (Louisville, KY), purified by HPLC as the acetate salt, and verified by mass spectrometry.

Membrane preparation—Confluent CHO and 3T3 cells were washed twice with cold PBS before collecting the cells by scraping into cold Homogenization Buffer (20 mM HEPES, 1 mM EDTA, 255 mM sucrose, pH 7.6). Cells were briefly sonicated to lyse then centrifuged 20 min at 10,000 × g, 4 °C. The precipitated membranes (P1) were resuspended in resuspension Buffer (20 mM HEPES, 1 mM EDTA, pH 7.6). The supernatants were transferred to fresh tubes and centrifuged 60 min at 41, 000 × g, 4 °C. These precipitated membranes (P2) were also resuspended in resuspension Buffer. Both membrane protein concentrations were determined by BCA assay (Pierce).

Crosslinking—3T3 and CHO membranes were diluted with PBS to 0.5 mg/mL protein. 1 mL of diluted membranes was aliquoted into a 96-well plate. An equivalent volume of TLQP-21 crosslink peptide was added to the diluted membranes and incubated for 10 min at room temperature. The 96-well plate was then placed on ice and transferred to the cold room for crosslinking. Crosslinking was achieved by a UV lamp (8 watt, 365 nm) for 30 min. Aliquots were collected from the 96-well plate and combined. In some cases (P2ppt), proteins were precipitated through addition of trichloroacetic acid to achieve a 6% solution. After 30 min incubation on ice, the samples were centrifuged to isolate the protein pellets. The protein pellets were washed twice with cold acetone and then resuspended in RIPA buffer (25 mM Tris base, 150 mM NaCl, pH 8.0, 1% deoxycholic acid, 1% Triton X-100).

Western Blotting—Aliquots of either the crosslinked P1 or P2 membrane solution or the solubilized precipitated membrane solution (P2ppt) were loaded onto 4-12% bis-TRIS gels and separated with MOPS buffer (Invitrogen) before transfer to nitrocellulose membranes. After blocking for 1 h in 5% milk in TBS-T, the membranes were washed 4 × 10 min with TBS-T and blotted with guinea pig anti-TLQP21 antibody (Possenti et al., 2012); 1:10,000 5% BSA) for 72 h at 4 °C, and then 90 min in anti-guinea pig IRDye 680RD (Li-Cor, 926-68077). The membranes were then scanned by Li-Cor Odyssey.

GPCR β-arrestin recruitment assay: G-protein independent

The assay was done as previously reported (Lin et al., 2013). Additional details appear in the Supplementary Methods.

Lipolysis and western blotting in 3T3L1 adipocytes

The 3T3-L1 cell line was obtained from the Minnesota Obesity Center. During proliferation these cells show a similar morphology to fibroblasts. Once 3T3-L1 fibroblast cells reach confluence they are exposed to an adipogenic cocktail including fetal bovine serum, dexamethasone, methylisobutylxanthine and insulin (Possenti et al., 2012; Green and Kehinde, 1975). Induction of differentiation triggers profound phenotypical changes, from elongated to spherical filled with lipid droplets displaying many morphological characteristics of adipocytes, as well as biochemical changes, expression of specific

adipogenic transcription factors and genes. At the fully differentiated stage these cells can be used to study adipocyte metabolism and function.

Lipolysis assay in 3T3 L1—At day 8 of differentiation 3T3-L1 adipocytes differentiated on 6-well plates were first starved for 3 hours in KRH with 1% BSA, then incubated with TLQP-21 in the presence and absence of specific agonists/antagonists, as clarified above, suspended in KRH with 4% BSA. Following 3 hours of incubation at 37°C and 5% CO_2, the media was collected and incubated at 60°C for 20 min to inactivate any residual enzymatic reaction activity. The cells were gathered for protein concentration or trypsinized for cell diameter and viability measurements. At least three independent experimental replicates were performed for each treatment.

Western blotting—Cells were from ATCC and differentiated as described above. Equivalent amounts of cell extracts (approximately 5×10^5 cells) were mixed with SDS-reducing sample buffer according to Invitrogen Nu PAGE (Invitrogen USA). For detailed procedures see [6]. Incubation with primary antibodies was performed overnight at 4°C with anti-Phospho-AMPK(Thr172) (Cell Signaling Technology (Beverly, MA, USA). Anti-Tubulin was a monoclonal antibody from Sigma. Secondary antibodies were donkey anti-rabbit or anti-mouse peroxidase-coupled (Amersham). A semi quantitative analysis of Western blots densitometry scan was performed using Scan Analysis software ImageJ. Data were analyzed with ANOVA followed by Tukey`s post hoc tests.

Supplementary Material

Refer to Web version on PubMed Central for supplementary material.

ACKNOWLEDGMENTS

Supported by the Minnesota Partnership for Biotechnology and Medical Genomic, Decade of Discovery in Diabetes Grant (AB), NIH/DK10249601 (AB), NIH R01DE021996 and NIH R21DA025170 (LV) and the NIMH Psychoactive Drug Screening Program (BLR and MFS). NMR experiments were carried out at the Minnesota NMR Center. 3T3L1 cells were provided by The Molecular & Cellular Basis of Obesity Core, Minnesota Obesity Center (5P30DK050456-18). We wish to thank D. Piomelli, G. Bottegoni, W. Rocchia, A. Lodola and M. Mor for important suggestions in various stages of the study, and I. Ninkovich, P. Petrocchi and M. Razzoli for technical help.

REFERENCES

Adessi C, Soto C. Converting a peptide into a drug: strategies to improve stability and bioavailability. Curr Med Chem. 2002; 9:963–78. [PubMed: 11966456]

Aguilar E, Pineda R, Gaytán F, Sánchez-Garrido MA, Romero M, Romero-Ruiz A, Ruiz-Pino F, Tena-Sempere M, Pinilla L. Characterization of the reproductive effects of the Vgf-derived peptide TLQP-21 in female rats: in vivo and in vitro studies. Neuroendocrinology. 2013; 98:38–50. [PubMed: 23485923]

Ames RS, Lee D, Foley JJ, Jurewicz AJ, Tornetta MA, Bautsch W, Settmacher B, Klos A, Erhard KF, Cousins RD, et al. Identification of a selective nonpeptide antagonist of the anaphylatoxin C3a receptor that demonstrates antiinflammatory activity in animal models. J Immunol. 2001; 166:6341–8. [PubMed: 11342658]

Ammoun S, Holmqvist T, Shariatmadari R, Oonk HB, Detheux M, Parmentier M, Akerman KE, Kukkonen JP. Distinct recognition of OX1 and OX2 receptors by orexin peptides. J Pharmacol Exp Ther. 2003; 305:507–14. [PubMed: 12606634]

Baker NA, Sept D, Joseph S, Holst MJ, McCammon JA. Electrostatics of nanosystems: application to microtubules and the ribosome. Proc Natl Acad Sci USA. 2001; 98:10037–41. [PubMed: 11517324]

Bartolomucci A, La Corte G, Possenti R, Locatelli V, Rigamonti AE, Torsello A, Bresciani E, Bulgarelli I, Rizzi R, Pavone F, et al. TLQP-21, a VGF-derived peptide, increases energy expenditure and prevents the early phase of diet-induced obesity. Proc Natl Acad Sci USA. 2006; 103:14584–9. [PubMed: 16983076]

Bartolomucci A, Possenti R, Mahata SK, Fischer-Colbrie R, Loh YP, Salton SR. The extended granin family: structure, function, and biomedical implications. Endocr Rev. 2011; 32:755–97. [PubMed: 21862681]

Beck-Sickinger AG, Wieland HA, Wittneben H, Willim KD, Rudolf K, Jung G. Complete L-alanine scan of neuropeptide Y reveals ligands binding to Y1 and Y2 receptors with distinguished conformations. Eur J Biochem. 1994; 225:947–58. [PubMed: 7957231]

Cassina V, Torsello A, Tempestini A, Salerno D, Brogioli D, Tamiazzo L, Bresciani E, Martinez J, Fehrentz JA, Verdié P, et al. Biophysical characterization of a binding site for TLQP-21, a naturally occurring peptide which induces resistance to obesity. Biochim Biophys Acta. 2013; 1828:455–60. [PubMed: 23122777]

Chen YC, Pristerá A, Ayub M, Swanwick RS, Karu K, Hamada Y, Rice AS, Okuse K. Identification of a receptor for neuropeptide VGF and its role in neuropathic pain. J Biol Chem. 2013; 288:34638–46. [PubMed: 24106277]

Choy LN, Rosen BS, Spiegelman BM. Adipsin and an endogenous pathway of complement from adipose cells. J Biol Chem. 1995; 267:12736–41. [PubMed: 1618777]

Engelke, F.; Steuernagel, S. Encyclopedia of Magnetic Resonance. John Wiley & Sons, Ltd; 2007. Cross Polarization in Rotating Solids: Spin-1/2 Nuclei..

Fairbanks CA, Peterson CD, Speltz RH, Riedl MS, Kitto KF, Dykstra JA, Braun PD, Sadahiro M, Salton SR, Vulchanova L. The VGF-derived peptide TLQP-21 contributes to inflammatory and nerve injury-induced hypersensitivity. Pain. 2014 in press.

Fargali S, Garcia AL, Sadahiro M, Jiang C, Janssen WG, Lin WJ, Cogliani V, Elste A, Mortillo S, Cero C, et al. The Granin VGF Promotes the Genesis of Secretory Vesicles, and Regulates Circulating Catecholamine Levels and Blood Pressure. FASEB J. 2014; 28:2120–33. [PubMed: 24497580]

Fargali S, Scherer T, Shin AC, Sadahiro M, Buettner C, Salton SR. Germline ablation of VGF increases lipolysis in white adipose tissue. J Endocrinol. 2012; 215:313–22. [PubMed: 22942234]

Fyfe CA, Wong-Moon KC, Huang Y, Grondey H. INEPT Experiments in Solid-State NMR. J Am Chem Soc. 1995; 117:10397–10398.

Gaboriaud C, Juanhuix J, Gruez A, Lacroix M, Darnault C, Pignol D, Verger D, Fontecilla-Camps JC, Arlaud GJ. The crystal structure of the globular head of complement protein C1q provides a basis for its versatile recognition properties. J Biol Chem. 2003; 278:46974–46982. [PubMed: 12960167]

Garcia AL, Han SK, Janssen WG, Khaing ZZ, Ito T, Glucksman MJ, Benson DL, Salton SR. A prohormone convertase cleavage site within a predicted alpha-helix mediates sorting of the neuronal and endocrine polypeptide VGF into the regulated secretory pathway. J Biol Chem. 2005; 280:41595–608. [PubMed: 16221685]

Grace CR, et al. Common and divergent structural features of a series of corticotropin releasing factor-related peptides. J Am Chem Soc. 2007; 129:16102–16114. [PubMed: 18052377]

Green H, Kehinde O. An established preadipose cell line and its differentiation in culture. II. Factors affecting the adipose conversion. Cell. 1975; 5:19–27. [PubMed: 165899]

Hahm S, Fekete C, Mizuno TM, Windsor J, Yan H, Boozer CN, Lee C, Elmquist JK, Lechan RM, Mobbs CV, Salton SR. VGF is required for obesity induced by diet, gold thioglucose treatment, and agouti and is differentially regulated in pro-opiomelanocortin-and neuropeptide Y-containing arcuate neurons in response to fasting. J Neurosci. 2002; 22:6929–38. [PubMed: 12177191]

Hahm S, Mizuno TM, Wu TJ, Wisor JP, Priest CA, Kozak CA, Boozer CN, Peng B, McEvoy RC, et al. Targeted deletion of the Vgf gene indicates that the encoded secretory peptide precursor plays a novel role in the regulation of energy balance. Neuron. 1999; 23:537–48. [PubMed: 10433265]

Hannedouche S, Beck V, Leighton-Davies J, Beibel M, Roma G, Oakeley EJ, Lannoy V, Bernard J, Hamon J, Barbieri S, et al. The identification of the C3a Receptor (C3AR1) as the target of the VGF derived peptide TLQP-21 in rodent cells. J Biol Chem. 2013; 288:27434–43. [PubMed: 23940034]

Hollenstein K, de Graaf C, Bortolato A, Wang MW, Marshall FH, Stevens RC. Insights into the structure of class B GPCRs. Trends Pharmacol Sci. 2014; 35:12–22. [PubMed: 24359917]

Hugli TE, Erickson BW. Synthetic peptides with the biological activities and specificity of human C3a anaphylatoxin. Proc Natl Acad Sci U S A. 1977; 74:1826–1830. [PubMed: 266705]

Jethwa PH, Warner A, Nilaweera KN, Brameld JM, Keyte JW, Carter WG, Bolton N, Bruggraber M, Morgan PJ, Barrett P, Ebling FJ. VGF-derived peptide, TLQP-21, regulates food intake and body weight in Siberian hamsters. Endocrinology. 2007; 148:4044–55. [PubMed: 17463057]

Karnik SS, Gogonea C, Patil S, Saad Y, Takezako T. Activation of G-protein-coupled receptors: a common molecular mechanism. Trends in Endocrinology and Metabolism. 2003; 14:431–437. [PubMed: 14580763]

Klos A, Wende E, Wareham KJ, Monk PN. International Union of Pharmacology. LXXXVII. Complement peptide C5a, C4a, and C3a receptors. Pharmacol Rev. 2013; 65:500–43. [PubMed: 23383423]

Kwan WH, van der Touw W, Paz-Artal E, Li MO, Heeger PS. Signaling through C5a receptor and C3a receptor diminishes function of murine natural regulatory T cells. J Exp Med. 2013; 210:257–68. [PubMed: 23382542]

Lin H, Sassano MF, Roth BL, Shoichet BK. A pharmacological organization of G protein-coupled receptors. Nature Met. 2013; 10:140–146.

Lo JC, Ljubicic S, Leibiger B, Kern M, Leibiger IB, Moede T, Kelly ME, Chatterjee Bhowmick, D. Murano I, Cohen P, Banks AS, Khandekar MJ, Dietrich A, Flier JS, Cinti S, Blüher M, Danial NN, Berggren PO, Spiegelman BM. Adipsin Is an adipokine that Improves β Cell Function in Diabetes. Cell. 2014; 158:41–53. [PubMed: 24995977]

Mamane Y, Chung Chan C, Lavallee G, Morin N, Xu LJ, Huang J, Gordon R, Thomas W, Lamb J, Schadt EE, et al. The C3a anaphylatoxin receptor is a key mediator of insulin resistance and functions by modulating adipose tissue macrophage infiltration and activation. Diabetes. 2009; 58:2006–17. [PubMed: 19581423]

Morrison KL, Weiss GA. Combinatorial alanine-scanning. Curr Opin Chem Biol. 2001; 5:302–307. [PubMed: 11479122]

Murage EN, Schroeder JC, Beinborn M, Ahn JM. Search for alpha-helical propensity in the receptor-bound conformation of glucagon-like peptide-1. Bioorganic & medicinal chemistry. 2008; 16:10106–10112. [PubMed: 18952440]

Neelamkavil S, Arison B, Birzin E, Feng JJ, et al. Replacement of Phe6, Phe7, and Phe11 of D-Trp8-somatostatin-14 with L-pyrazinylalanine. Predicted and observed effects on binding affinities at hSST2 and hSST4. An unexpected effect of the chirality of Trp8 on NMR spectra in methanol. J Med Chem. 2005; 48:4025–30. [PubMed: 15943475]

Nettesheim DG, Edalji RP, Mollison KW, Greer J, Zuiderweg ER. Secondary structure of complement component C3a anaphylatoxin in solution as determined by NMR spectroscopy: differences between crystal and solution conformations. Proc Natl Acad Sci U S A. 1988; 85:5036–5040. [PubMed: 3260670]

Pal K, Melcher K, Xu HE. Structure and mechanism for recognition of peptide hormones by Class B G-protein-coupled receptors. Acta pharmacologica Sinica. 2012; 33:300–311. [PubMed: 22266723]

Parthier C, Reedtz-Runge S, Rudolph R, Stubbs MT. Passing the baton in class B GPCRs: peptide hormone activation via helix induction? Trends Biochem Sci. 2009; 34:303–310. [PubMed: 19446460]

Pellecchia M, Bertini I, Cowburn D, Dalvit C, Giralt E, Jahnke W, James TL, Homans SW, Kessler H, Luchinat C, et al. Perspectives on NMR in drug discovery: a technique comes of age. Nat Rev Drug Discov. 2008; 7:738–45. [PubMed: 19172689]

Possenti R, Muccioli G, Petrocchi P, Cero C, Cabassi A, Vulchanova L, Riedl MS, Manieri M, Frontini A, Giordano A, et al. Characterization of a novel peripheral pro-lipolytic mechanism in mice: role of VGF-derived peptide TLQP-21. Biochem J. 2012; 441:511–22. [PubMed: 21880012]

Razzoli M, Bo E, Pascucci T, Pavone F, D'Amato FR, Cero C, Sanghez V, Dadomo H, Palanza P, Parmigiani S, et al. Implication of the VGF-derived peptide TLQP-21 in mouse acute and chronic stress responses. Behav Brain Res. 2012; 229:333–9. [PubMed: 22289198]

Reid RC, Yau MK, Singh R, Hamidon JK, Reed AN, Chu P, Suen JY, Stoermer MJ, Blakeney JS, Lim J, et al. Downsizing a human inflammatory protein to a small molecule with equal potency and functionality. Nat Commun. 2013; 4:2802. [PubMed: 24257095]

Rizzi R, Bartolomucci A, Moles A, D'Amato F, Sacerdote P, Levi A, La Corte G, Ciotti MT, Possenti R, Pavone F. The VGF-derived peptide TLQP-21: a new modulatory peptide for inflammatory pain. Neurosci Lett. 2008; 441:129–33. [PubMed: 18586396]

Roglic A, Prossnitz ER, Cavanagh SL, Pan Z, Zou A, Ye RD. cDNA cloning of a novel G protein-coupled receptor with a large extracellular loop structure. Biochim Biophys Acta. 1996; 1305:39–43. [PubMed: 8605247]

Roy C, Paglialunga S, Fisette A, Schrauwen P, Moonen-Kornips E, St-Onge J, Hesselink MK, Richard D, Joanisse DR, Cianflone K. Shift in metabolic fuel in acylation-stimulating protein-deficient mice following a high-fat diet. Am J Physiol Endo Metabol. 2008; 294:E1051–E1059.

Schwarzinger S, Kroon GJ, Foss TR, Wright PE, Dyson HJ. Random coil chemical shifts in acidic 8 M urea: implementation of random coil shift data in NMRView. J Biomol NMR. 2000; 18:43–8. [PubMed: 11061227]

Schwieters CD, Kuszewski JJ, Tjandra N, Clore GM. The Xplor-NIH NMR molecular structure determination package. J Magn Reson. 2003; 160:65–73. [PubMed: 12565051]

Severini C, La Corte G, Improta G, Broccardo M, Agostini S, Petrella C, Sibilia V, Pagani F, Guidobono F, Bulgarelli I, et al. In vitro and in vivo pharmacological role of TLQP-21, a VGF-derived peptide, in the regulation of rat gastric motor functions. Br J Pharmacol. 2009; 157:984–93. [PubMed: 19466987]

Shoichet BK, Kobilka BK. Structure-based drug screening for G-protein-coupled receptors. Trends Pharmacol Sci. 2012; 33:268–72. [PubMed: 22503476]

Stephens SB, Schisler JC, Hohmeier HE, An J, Sun AY, Pitt GS, Newgard CB. A VGF-derived peptide attenuates development of type 2 diabetes via enhancement of islet β-cell survival and function. Cell Metab. 2012; 16:33–43. [PubMed: 22768837]

Takahashi M, Moriguchi S, Ikeno M, Kono S, Ohata K, Usui H, Kurahashi K, Sasaki R, Yoshikawa M. Studies on the ileum-contracting mechanisms and identification as a complement C3a receptor agonist of oryzatensin, a bioactive peptide derived from rice albumin. Peptides. 1996; 17:5–12. [PubMed: 8822503]

Takahashi M, Moriguchi S, Suganuma H, Shiota A, Tani F, Usui H, Kurahashi K, Sasaki R, Yoshikawa M. Identification of casoxin C, an ileum-contracting peptide derived from bovine kappa-casein, as an agonist for C3a receptors. Peptides. 1997; 18:329–36. [PubMed: 9145417]

Vale W, Spiess J, Rivier C, Rivier J. Characterization of a 41-residue ovine hypothalamic peptide that stimulates secretion of corticotropin and beta-endorphin. Science. 1981; 213:1394–1397. [PubMed: 6267699]

Veglia, G., et al. Comprehensive Biophysics. Vol. 1: Biophysical Techniques for Structural Characterization of Macromolecules Ch 1.11. Elsevier; 2012.

Watson E, Hahm S, Mizuno TM, Windsor J, Montgomery C, Scherer PE, Mobbs CV, Salton SR. VGF ablation blocks the development of hyperinsulinemia and hyperglycemia in several mouse models of obesity. Endocrinology. 2005; 146:5151–63. [PubMed: 16141392]

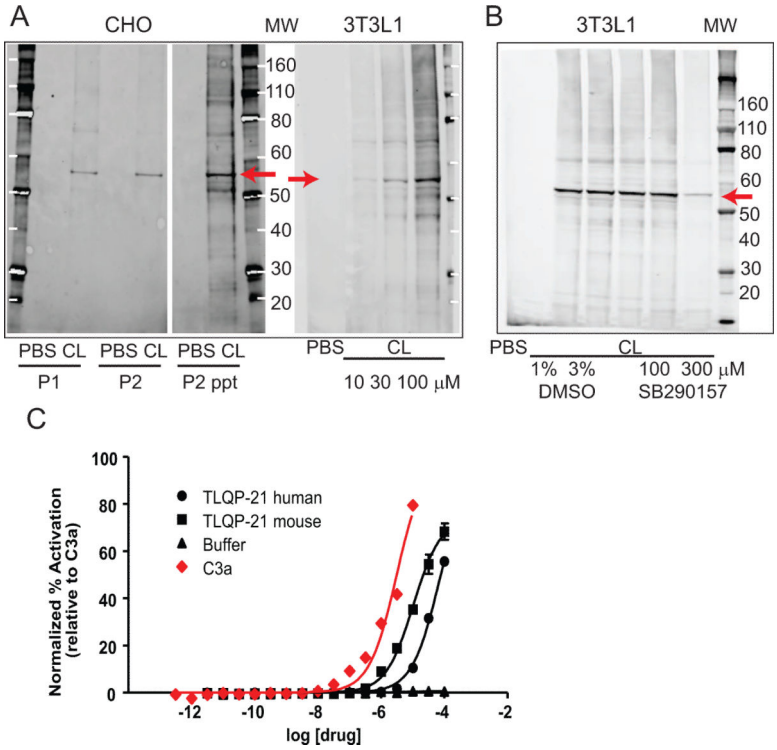

Figure 1. TLQP-21 binding in 3T3L1 and CHO cells and activity at the C3aR1

A) Photoactivated crosslinking of a modified TLQP-21 peptide (CL) in CHO and 3T3 cells. CHO membranes were treated with PBS or CL (100 μM). A band of ~56 kDa was observed with anti-TLQP21 in membrane fractions P1and P2 from CL-treated but not PBS-treated membranes. Labeling remained in the protein pellet when P2 membranes were TCA-precipitated (P2 ppt). P2 membranes from 3T3 cells were treated with PBS or increasing concentrations of CL. **B**) Crosslinking of a modified TLQP-21 peptide (CL) to membranes prepared from 3T3 cells is reduced in the presence of the C3aR1 antagonist SB290157. Lanes 2 and 3 show that crosslinking is not affected by DMSO used to dissolve SB290157. **C**) The β-arrestin recruitment assay showed that TLQP-21 is an agonist for the human C3aR1, similarly to the human C3a peptide. The mouse TLQP-21 has higher potency than the human TLQP-21.

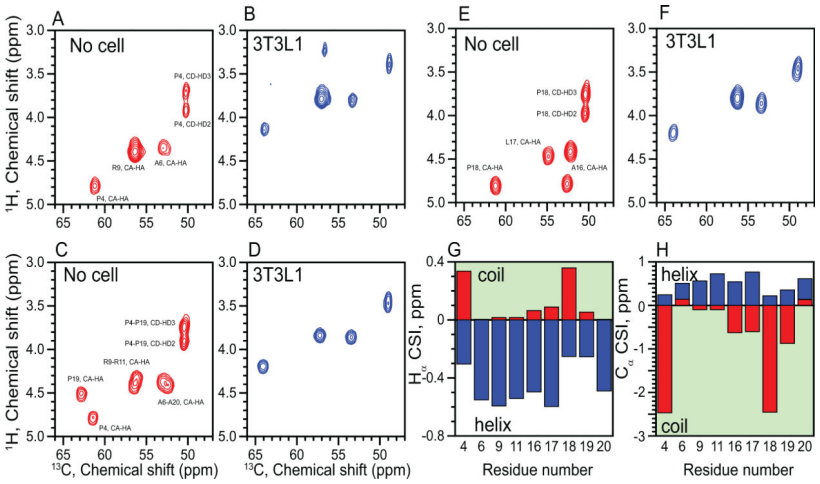

Figure 2. Structural analysis of TLQP-21 in presence of target 3T3L1 cells

Overlay spectra of refocused INEPT spectrum of TLQP-21 ^{13}C and ^{15}N labeled at P_4-R_6-A_9 (**A,B**), P_4-A_6-R_9-R_{11}-P_{19}-A_{20} (**C,D**) or A_{16}-L_{17}-P_{18} (**E,F**) with resonance assignments indicated. Experiments were performed in buffer (**A,C,E**) or in the presence of 3T3L1 cells after 24 hour incubation at 37°C (**B,D,F**). **G,H**. Chemical shift index of TLQP-21 in buffer (red) or in the presence of 3T3L1 cells (blue) (Schwarzinger, et al., 2000).

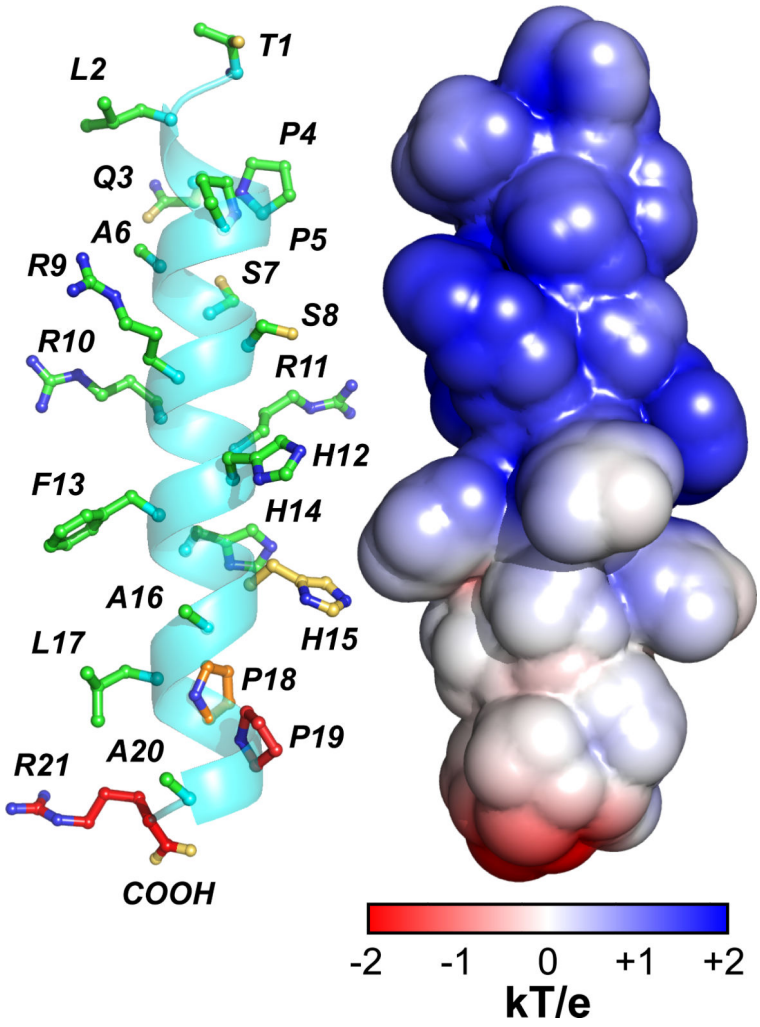

Figure 3. A structural model of TLQP-21 upon receptor binding

The backbone conformation was obtained with XPLOR-NIH software (Schwieters et al., 2003) constraining the dihedral angles of the residues showing helical chemical shifts. The conformation of the side chains is arbitrary. Electrostatic surface calculated with APBS (Baker et al., 2001) illustrates the positively charged N-terminal domain of TLQP-21 and primarily neutral C-terminal domain.

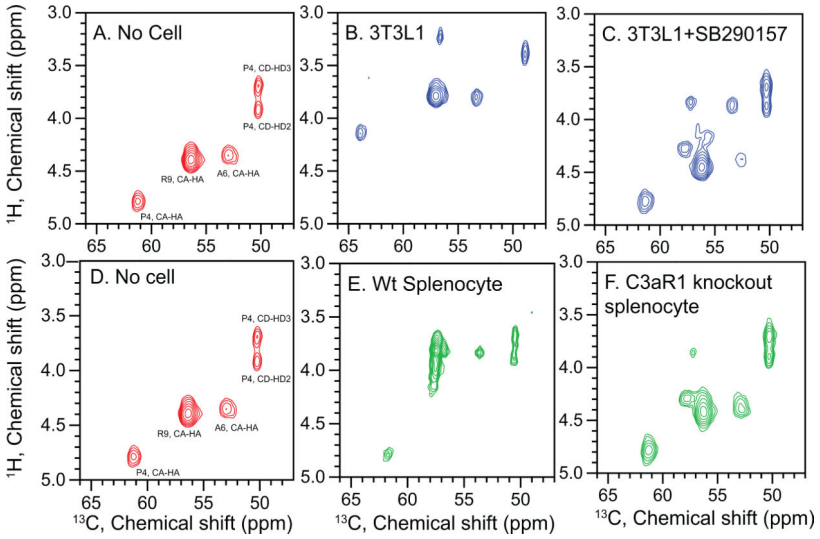

Figure 4. Structural analysis of TLQP-21 in presence of C3aR1 knockout cells and a C3aR1 antagonist

Refocused INEPT spectra of TLQP-21, labeled with ^{13}C and ^{15}N at P_4-A_6-R_9 with resonance assignments indicated. Experiments were performed in buffer (**A,D**), in the presence of 3T3L1 cells (**B**), in the presence of 3T3L1 cells incubated with the C3aR1 antagonist SB290157 (**C**), in the presence of splenocytes derived from wild type (**E**) or in the presence of splenocytes derived from a C3aR1 knockout mice (**F**).

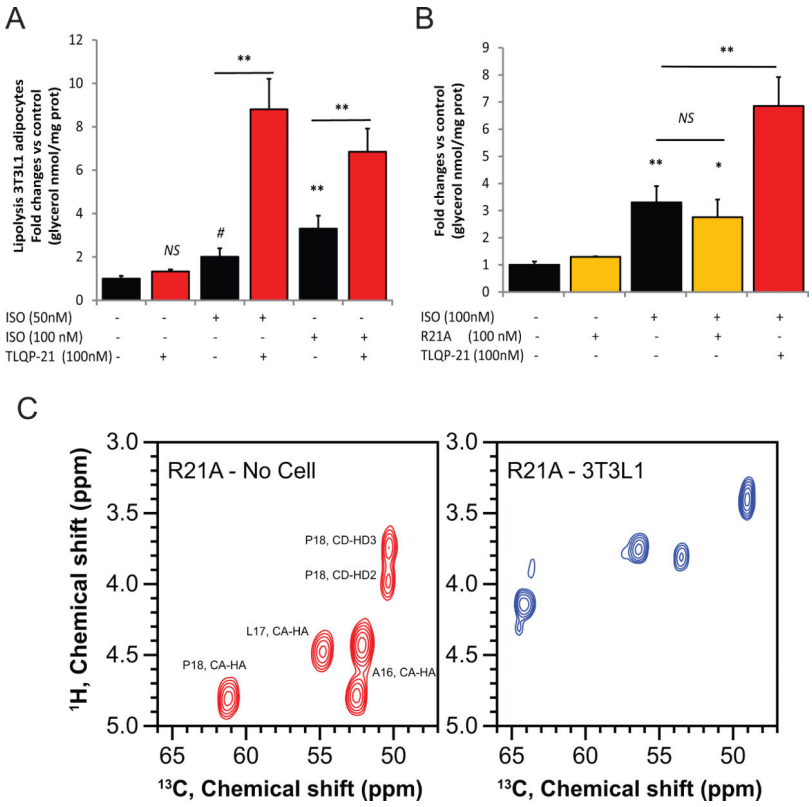

Figure 5. TLQP-21 but not R21A mutant enhances lipolysis in 3T3L1

A) TLQP-21 potentiates lipolysis induced by the β-adrenergic receptor agonist isoproterenol (ISO) ($F(5,65)=62.1$, $p<0.0001$). **B**) Unlike TLQP-21, the R21A mutant peptide does not potentiate isoproterenol-induced lipolysis in 3T3L1 adipocytes ($F(5,65)=33.4$, $p<0.00001$). **C**) Refocused INEPT spectra of R21A mutant, labeled with ^{13}C and ^{15}N at A_{16}-L_{17}-P_{18} with resonance assignments indicated. Experiments were performed in buffer (left panel) or in the presence of 3T3L1 cells (right panel). *$p<0.05$, ** $p<0.001$.

Table 1

Contractile activity on rat stomach fundus exerted by TLQP-21 mutants (mutation highlighted in bold).

Peptide	Activity % of TLQP-21 (average ± SEM)
TLQPPASSRRRHFHHALPPAR	100
TLQPPASSRRR	inactive
HFHHALPPAR	2.6±4***
TLQPPASSRRR**A**FHHALPPAR	95±4
TLQPPASSRRRH**A**HHALPPAR	88±9
TLQPPASSRRRHF**A**HALPPAR	91±5
TLQPPASSRRRHFH**A**ALPPAR	84±10
TLQPPASSRRRHFHHAL**A**PAR *(P18A)*	65±7 *
TLQPPASSRRRHFHHALP**A**AR *(P19A)*	19±4***
TLQPPASSRRRHFHHALPPA**A** *(R21A)*	inactive
TLQPPASSRRRHFHHALPPAR-**NH2**	inactive
TLQPPSALRRRHYHHALPPSR *(human)*	20±9**

* p>0.5

** <0.01

*** <0.001.